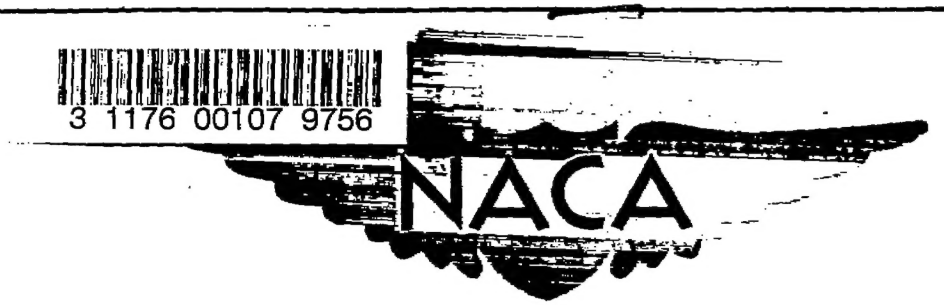

RESEARCH MEMORANDUM

PRELIMINARY MEASUREMENTS OF TURBULENCE AND TEMPERATURE FLUCTUATIONS BEHIND A HEATED GRID

By A. L. Kistler, V. O'Brien, and S. Corrsin

The Johns Hopkins University

NATIONAL ADVISORY COMMITTEE
FOR AERONAUTICS

WASHINGTON

June 10, 1954

NATIONAL ADVISORY COMMITTEE FOR AERONAUTICS

RESEARCH MEMORANDUM

PRELIMINARY MEASUREMENTS OF TURBULENCE AND TEMPERATURE FLUCTUATIONS BEHIND A HEATED GRID

By A. L. Kistler, V. O'Brien, and S. Corrsin

SUMMARY

Preliminary measurements have been made of velocity and temperature fluctuations in the flow behind a heated grid in a uniform airstream. Temperature correlation shows a reasonable degree of isotropy, and the temperature fluctuations die out at large distances more slowly than the turbulence, as has been predicted theoretically under some strongly simplifying postulates.

INTRODUCTION

A comparison between the correlation equations for concomitant (incompressible isotropic velocity and temperature fields showed marked differences attributable to the fact that velocity is a vector while temperature is a scalar (refs. 1, 2, and 3).[1] The relative decay rates were calculated under strongly simplifying assumptions, and the relative "microscales" and relative wave numbers characterizing the very fine structures were deduced in terms of the Prandtl number of the fluid. Since the theoretical predictions are essentially conjectural, it is necessary to get at some facts through measurement.

A hot grid with thermal mesh equal to momentum mesh is as simple as any, so this configuration was selected, with the expectation that approximate equality of integral scales would be obtained.

The analysis of reference 1 suggests that the flow with equal integral scales for velocity and temperature fields may not be the simplest case analytically, but could be the simplest for experimental realization.

[1]As pointed out in references 1 and 2, the work applies equally well to isotropic turbulent mixing between two different components provided that the molecular mass transfer coefficient is nearly constant over the concentration range encountered.

This report describes the preliminary data. It is hoped that with improved grid and measuring procedure, less scattered results will be gotten in the measurements now in progress.

The investigation was conducted at the Johns Hopkins University under the sponsorship and with the financial assistance of the National Advisory Committee for Aeronautics.

SYMBOLS

$E_1(k_1)$	one-dimensional power spectrum of u-fluctuations
$E_\vartheta(k_1)$	one-dimensional power spectrum of ϑ-fluctuations
f	"longitudinal" double velocity correlation, $\dfrac{\overline{u(x,y,z)u(x+\xi,y,z)}}{u'(x)u'(x+\xi)}$
g	"lateral" double velocity correlation, $\dfrac{\overline{u(x,y,z)u(x,y+\eta,z)}}{u'^2(x)}$
k_1	wave number in x-direction
$k_c, {}_\vartheta k_c$	spectral "cut off" for $E_1(k_1)$ and $E_\vartheta(k_1)$, respectively
L, L_1, L_ϑ	integral scales of g, f, and m, respectively
M, M_ϑ	grid mesh size for momentum and heat $(M = M_\vartheta = 1$ in.$)$
m	temperature correlation
r	space interval
t	time
u	turbulent velocity fluctuation in x-direction
x,y,z	Cartesian space coordinates; x is alined with mean flow
γ	thermal diffusivity coefficient, $K/\rho C_p$, where K is thermal conductivity coefficient, ρ is density, and C_p is specific heat at constant pressure

η	space interval in y-direction, $\equiv\Delta y$
ϑ	temperature fluctuation
$\lambda,\lambda_\vartheta$	dissipation scales for velocity and temperature fluctuations, respectively
ν	kinematic viscosity coefficient
ξ	space interval in x-direction, $\equiv\Delta x$
σ	Prandtl number, ν/γ

EQUIPMENT AND PROCEDURES

Approximately isotropic turbulence is produced at some distance behind a square-mesh biplane of grid of $\frac{1}{4}$-inch round wooden dowels spaced 1 inch on centers. The grid is set at the upstream end of the working section of the wind tunnel sketched in figure 1.

As a first method of generating isotropic temperature fluctuations in this turbulence, a grid of Nichrome heating wires was introduced about $1\frac{1}{2}$ inches upstream of the dowel grid, with wires geometrically in phase, that is, alined so that their wakes passed over the rods (fig. 2). In this way the hot air passed through the turbulence-generating shear zones of the main grid, so that temperature and velocity fluctuations were produced in the same local neighborhoods.

Turbulence and temperature fluctuation measurements were made with the hot-wire anemometry equipment described in reference 4. The experimental procedures for simultaneous velocity and temperature fluctuations are given in reference 5.

The measurements were all made at a mean speed of 14 feet per second and a mean temperature rise (across the grid) of about 5° C. The actual heating wire temperatures were about 500° C. The resulting temperature fluctuations were inconveniently small, but this insured negligible influence of density variations upon the fully developed turbulent velocity field - as attested by both turbulence level and correlation measurements.

Because of the extremely small temperature fluctuations it was necessary to use unusually high resistance hot-wires, 0.0001-inch platinum of about 90 ohms resistance. This wire was set in the form of a V (with

plane perpendicular to mean flow) in order to reduce the error due to finite wire length. The high resistance necessitated correction for heating current fluctuations when the system was operated as an anemometer.

As has been found before (ref. 6), the velocity field was not quite isotropic within the precision of measurement: $v' \approx 0.9u'$ at $x/M = 100$; but this is apparently insufficient anisotropy to cause difficulties. A reasonable degree of isotropy in the thermal field is indicated by the approximate equality of longitudinal and lateral temperature correlation functions (fig. 5).

For convenience the spectrum was measured without heating, after it had been determined that the u'-levels and correlations were not appreciably changed by the heating.

The temperature spectrum was measured with "mixed" sensitivity, that is, wire temperature set for the same order of response to velocity and temperature. This was done because under resistance-thermometer conditions (heating current < 1 milliampere) the signal was of the order of the amplifier noise level over most of the frequency range.

With mixed sensitivity the hot-wire responds to both velocity and temperature spectra, which must be "separated." Simple superposition of the two energy spectra follows from the assumption that all "harmonics" of the two spectra are uncorrelated. Since $\overline{u_1 \vartheta} = 0$ in this field, such an assumption seems reasonable. Then the temperature spectrum is obtained by subtracting the (unheated grid) velocity spectrum from the mixed spectrum.

A Hewlett-Packard model 300 A wave analyzer was used as variable frequency band pass filter.

No correction has been made for wire length.

EXPERIMENTAL RESULTS

The velocity and temperature decay curves are plotted in figures 3 and 4, respectively. A number of runs are given for each to indicate the repeatability of the data as well as the equality of hot- and cold-grid flows (fig. 3) and the consistency of two difference measuring methods (fig. 4). The u'-values are a bit lower than those obtained behind a similar grid in a different wind tunnel (ref. 6).

Figure 5 shows longitudinal and lateral temperature correlations at $x/M = 69$. Of course it was necessary to keep the downstream probe out of the wake of the upstream one, so the Δx coordinate is actually

inclined to the x-axis by about 5°. The two sets of points match fairly well, indicating that the temperature field is not far from isotropy.

Figures 6 and 7 compare these curves with the corresponding velocity correlations. The close agreement of the longitudinal cases is especially noteworthy.

The experimental scatter is too great to permit a determination of the dissipative scales ("microscales") by graphical fitting of parabolas to the vertices of these correlation data. However, the integral scales have been calculated:

$$\left.\begin{aligned} L &\equiv \int_0^\infty g(\eta)\, d\eta \\ L_1 &\equiv \int_0^\infty f(\xi)\, d\xi \\ L_\vartheta &\equiv \int_0^\infty m(r)\, dr \end{aligned}\right\} \quad (1)$$

where $f(r)$ and $g(r)$ are the Kármán-Howarth notation so that

$$f(\xi) \equiv \frac{\overline{u(x,y,z)u(x+\xi,y,z)}}{u'(x)u'(x+\xi)}$$

$$g(\eta) \equiv \frac{\overline{u(x,y,z)u(x,y+\eta,z)}}{\overline{u^2(x)}}$$

Also

$$m(\xi) \equiv \frac{\overline{\vartheta(x,y,z)\vartheta(x+\xi,y,z)}}{\vartheta'(x)\vartheta'(x+\xi)}$$

and

$$m(\eta) \equiv \frac{\overline{\vartheta(x,y,z)\vartheta(x,y+\eta,z)}}{\overline{\vartheta^2(x)}}$$

are the longitudinal and lateral temperature correlation coefficient functions.

The results are

$$\left.\begin{aligned} L &= 0.40 \text{ in.} \\ L_1 &= 0.70 \text{ in.} \\ L_\vartheta &= \begin{cases} 0.66 \text{ in., laterally} \\ 0.68 \text{ in., longitudinally} \end{cases} \end{aligned}\right\} \quad (2)$$

In passing one notes that $\frac{L}{L_1} = 0.57 \neq 0.50$, the value corresponding to exactly isotropic turbulence. Since M, the momentum grid mesh, and M_ϑ, the heat grid mesh, are both 1.0 inch, the values in equations (2) are also L/M, L_1/M, and L_ϑ/M_ϑ, respectively.

The time spectra of ϑ and u at $x/M = 23$ were determined as described in the previous section and are given in figure 8. These may be considered good approximations to the one-dimensional longitudinal space spectra, except perhaps for the lowest wave number range (refs. 7 and 8). The sketched curves indicate a possible trend, but should not be taken seriously; within the experimental precision there is no significant difference. The circuit noise has been subtracted out for both sets of data.

These spectra have been used for approximate calculation of the dissipative scales of velocity and temperature fields:

$$\frac{1}{\lambda^2} = \int_0^\infty k_1^2 E_1(k_1)\, dk_1 \quad (3)$$

$$\frac{1}{\lambda_\vartheta^2} = \frac{1}{2}\int_0^\infty k_1^2 E_\vartheta(k_1)\, dk_1 \tag{4}$$

The results of graphical computation are

$$\left.\begin{aligned} \lambda_\vartheta &= 0.26 \text{ in.} \\ \lambda &= 0.19 \text{ in.} \end{aligned}\right\} \tag{5}$$

at $x/M = 23$.

With the assumption that velocity and temperature fields are sufficiently near to isotropy $\lambda(x)$ and $\lambda_\vartheta(x)$ can be calculated from the intensity traverses, as indicated in the next section. The resulting faired curves are plotted in figure 9, with the above values spotted in.

COMPARISON WITH THEORY

Of course the theories of isotropic turbulence and of isotropic scalar fluctuations in isotropic turbulence are still unsolved; in fact they have not even been formulated in a determinate way. Nevertheless, a number of consequences of isotropy have been inferred, including some particular (and relatively simple) forms of the averaged differential equations. Of especial interest here are the so-called "decay equations." For isotropic fields decaying in time, there are (refs. 1 and 9)

$$\frac{d\overline{u^2}}{dt} = -10\nu \frac{\overline{u^2}}{\lambda^2} \tag{6}$$

and

$$\frac{d\vartheta^2}{dt} = -12\gamma \frac{\overline{\vartheta^2}}{\lambda_\vartheta^2} \tag{7}$$

The actual experiments are done in steady state behind a grid with the various averaged quantities depending upon x instead of t. Taylor (ref. 9) has pointed out, in effect, that if these vary sufficiently

slowly with x equation (6) can be applied to the grid flow with the substitution $x/\overline{U} \doteq t$.[2] The same holds for equation (7), so that

$$\frac{d\overline{u^2}}{dx} \doteq -10 \frac{\nu}{\overline{U}} \frac{\overline{u^2}}{\lambda^2} \tag{8}$$

$$\frac{d\overline{\vartheta^2}}{dx} \doteq -12 \frac{\gamma}{\overline{U}} \frac{\overline{\vartheta^2}}{\lambda_\vartheta{}^2} \tag{9}$$

These two equations permit calculation of $\lambda(x)$ and $\lambda_\vartheta(x)$ from the experimental data on $u'(x)$ and $\vartheta'(x)$, as mentioned at the end of the previous section. The faired results are drawn in figure 9. The appreciable disagreement at $x/M = 23$ between λ's calculated from decay and from spectra is indicative of inaccurate spectra (the less accurate of the two kinds of data) and/or of appreciable deviation from isotropy this close to the grid.

The ratio $\lambda_\vartheta/\lambda$ varies almost linearly from 1.23 at $x/M = 25$ to 1.58 at $x/M = 100$ (fig. 9). The only other measurement of this ratio was on the axis of a heated round turbulent jet (ref. 4), where the value was about 1.34.

In reference 1 it is shown that for two special "kinds" of isotropic fields this ratio has the same simple value:

$$\frac{\lambda_\vartheta}{\lambda} = \sqrt{\frac{2}{\sigma}} \tag{10}$$

where σ is the Prandtl number ν/γ. The two kinds of isotropic fields are:

(a) Reynolds and Peclet numbers are so small that the convective effects are negligible for both heat and momentum. Therefore this is not really turbulence in the ordinary sense.

(b) Reynolds and Peclet numbers are both very large and each field is assumed to have a completely "self-preserving" correlation function during decay. In this model, due to Von Kármán (ref. 10), the dissipation

---

[2] In fact, this requires perhaps more justification than given by Taylor or by Kármán and Howarth. This has been discussed at a seminar lecture at M.I.T., May 1952, and printed copies are available from the Aeronautics Department of The Johns Hopkins University: "Remarks on the Comparison of Grid-Produced Turbulence With the Theory of Isotropic Turbulence," by S. Corrsin.

and conduction terms of the two correlation equations are neglected, but decay is indirectly included by substitution of the decay equations into terms of the correlation equation.

Equation (10) can also be deduced by an approach somewhat different from the above:

Assume the Reynolds and Peclet numbers so high that the "inertial subranges" $\left(\text{with } E_1(k_1) \text{ and } E_\vartheta(k_1) \text{ both } \sim k_1^{-5/3}\right)$ are sufficiently extensive to permit the approximations (ref. 2)

$$\left.\begin{aligned} E_1(k_1) &\sim k_1^{-5/3} \quad \text{when} \quad k_o < k_1 < k_c \\ &= 0 \quad \text{elsewhere} \\ E_\vartheta(k_1) &\sim k_1^{-5/3} \quad \text{when} \quad {}_\vartheta k_o < k_1 < {}_\vartheta k_c \\ &= 0 \quad \text{elsewhere} \end{aligned}\right\} \tag{11}$$

The "cut off" wave number k_c is just the inverse of Kolmogoroff's microscale,

$$k_c = \frac{2\pi}{\eta} \tag{12}$$

and ${}_\vartheta k_c$ is the analogous thermal quantity (ref. 2)

$${}_\vartheta k_c = \frac{2\pi}{\eta_\vartheta} \tag{13}$$

In reference 2 it was shown that

$$\frac{{}_\vartheta k_c}{k_c} = \sigma^{3/4} \tag{14}$$

Substituting equations (11), (13), and (14) into (3) and (4) and neglecting $k_o^{2/3}$ relative to $k_c^{2/3}$ and ${}_\vartheta k_o^{2/3}$ relative to ${}_\vartheta k_c^{2/3}$, there results

$$\frac{\lambda_\vartheta^2}{\lambda^2} \approx \left(\frac{k_o}{\vartheta k_o}\right)^{2/3} \frac{2}{\sigma} \tag{15}$$

If one now restricts to fields in which the thermal large structure is roughly equal to the velocity large structure (as in these experiments), $k_o \approx \vartheta k_o$, and one arrives again at equation (10).

In fact, none of the three sets of assumptions leading to equation (10) is directly applicable to these experiments. The Reynolds and Peclet numbers are not low enough for case (a) and not high enough for the other two cases. Furthermore, it is known that the correlation functions of velocity do not remain completely similar during decay (ref. 11). The important conjecture to be made is that a result encountered under such divergent sets of assumptions may have approximate validity in a wide range of situations - perhaps including the actual one.

Taking $\sigma = 0.72$ for air, equation (10) gives

$$\frac{\lambda_\vartheta}{\lambda} \approx 1.67$$

which is in reasonable agreement with the downstream values computed from the decay data (fig. 9).

The $\lambda_\vartheta/\lambda$ curve is just a particular way of displaying the decay data. Two other ways are instructive: Figure 10 shows the variation in Reynolds and Peclet numbers

$$\left.\begin{aligned} R_\lambda &\equiv \frac{u'\lambda}{\nu} \\ P_{\lambda_\vartheta} &\equiv \frac{u'\lambda_\vartheta}{\gamma} \end{aligned}\right\} \tag{16}$$

The apparent constancy of P_{λ_ϑ} is evident. Figure 11 shows the relative decay rates of temperature fluctuations and velocity fluctuations. For small values of x/M they die out at about the same rate, but for larger values of x/M ϑ' dies out at a decidedly lower rate than does u'. For fully isotropic fields the ratio of equation (7) to equation (6) gives

$$\frac{d\vartheta'/\vartheta'}{du'/u'} = \frac{6}{5\sigma}\left(\frac{\lambda}{\lambda_\vartheta}\right)^2 \tag{17}$$

and if equation (10) holds

$$\frac{d\vartheta'}{\vartheta'}\frac{u'}{du'} = \frac{3}{5} \tag{18}$$

which is very close to the measured results at large values of x/M. This is just another way of showing that $\lambda_\vartheta/\lambda$ does approach the value in equation (10).

In the absence of more complete data, no attempt has been made to compare the individual decay rates of ϑ' and u' with the theoretical predictions that can be obtained by a variety of postulates.

CONCLUSIONS

The principal conclusions to be drawn from the foregoing results on measurements of turbulence and temperature fluctuations behind a heated grid are that:

1. It is experimentally feasible to set up and measure concomitant velocity and temperature fluctuation fields downstream of a heated grid.

2. The two fields are moderately isotropic sufficiently far downstream.

3. Also, sufficiently far downstream, the dissipation scale ratio is approximately given by

$$\frac{\lambda_\vartheta}{\lambda} \approx \sqrt{\frac{2}{\sigma}}$$

a value deduced theoretically under widely divergent postulates, none of which corresponds closely to the present experimental conditions.

4. As a consequence of conclusions 2 and 3, far enough from the grid the temperature fluctuations die out more slowly than velocity fluctuations:

$$\vartheta'(x) \sim \left[u'(x)\right]^{3/5}$$

corresponding to equation (18).

The Johns Hopkins University,
Baltimore 18, Md., January 13, 1954.

REFERENCES

1. Corrsin, Stanley: The Decay of Isotropic Temperature Fluctuations in an Isotropic Turbulence. Jour. Aero. Sci., vol. 18, no. 6, June 1951, pp. 417-423.

2. Corrsin, S.: On the Spectrum of Isotropic Temperature Fluctuations in an Isotropic Turbulence. Jour. Appl. Phys., vol. 22, no. 4, Apr. 1951, pp. 469-473.

3. Obukhov, A. M.: Structure of the Temperature Field in Turbulent Flow. Izvestiia Akad. Nauk S.S.S.R., Ser. Geogr. Geofiz., vol. 13, no. 1, 1949, pp. 58-69. (In Russian, translated by U. S. Army Chemical Corps, Camp Detrick.)

4. Corrsin, Stanley, and Uberoi, Mahinder S.: Spectra and Diffusion in a Round Turbulent Jet. NACA Rep. 1040, 1951. (Supersedes NACA TN 2124.)

5. Corrsin, Stanley: Extended Applications of the Hot-Wire Anemometer. NACA TN 1864, 1949. (Précis in Rev. Sci. Instr., vol. 18, no. 7, July 1947, pp. 469-471.)

6. Corrsin, S.: Decay of Turbulence Behind Three Similar Grids. A.E. Dissertation, C.I.T., June 1942.

7. Uberoi, Mahinder S., and Corrsin, Stanley: Diffusion of Heat From a Line Source in Isotropic Turbulence. NACA Rep. 1142, 1953. (Supersedes NACA TN 2710.)

8. Lin, C. C.: On Taylor's Hypothesis and the Acceleration Terms in the Navier-Stokes Equation. Quart. Appl. Math., vol. X, no. 4, Jan. 1953, pp. 295-306.

9. Taylor, G. I.: Statistical Theory of Turbulence. Parts I-IV. Proc. Roy. Soc. (London), Ser. A, vol. 151, no. 873, Sept. 2, 1935, pp. 421-478.

10. De Kármán, Theodore, and Howarth, Leslie: On the Statistical Theory of Isotropic Turbulence. Proc. Roy. Soc. (London), Ser. A, vol. 164, no. 917, Jan. 21, 1938, pp. 192-215.

11. Batchelor, G. K.: Energy Decay and Self-Preserving Correlation Functions in Isotropic Turbulence. Quart. Appl. Math., vol. VI, no. 2, July 1948, pp. 97-116.

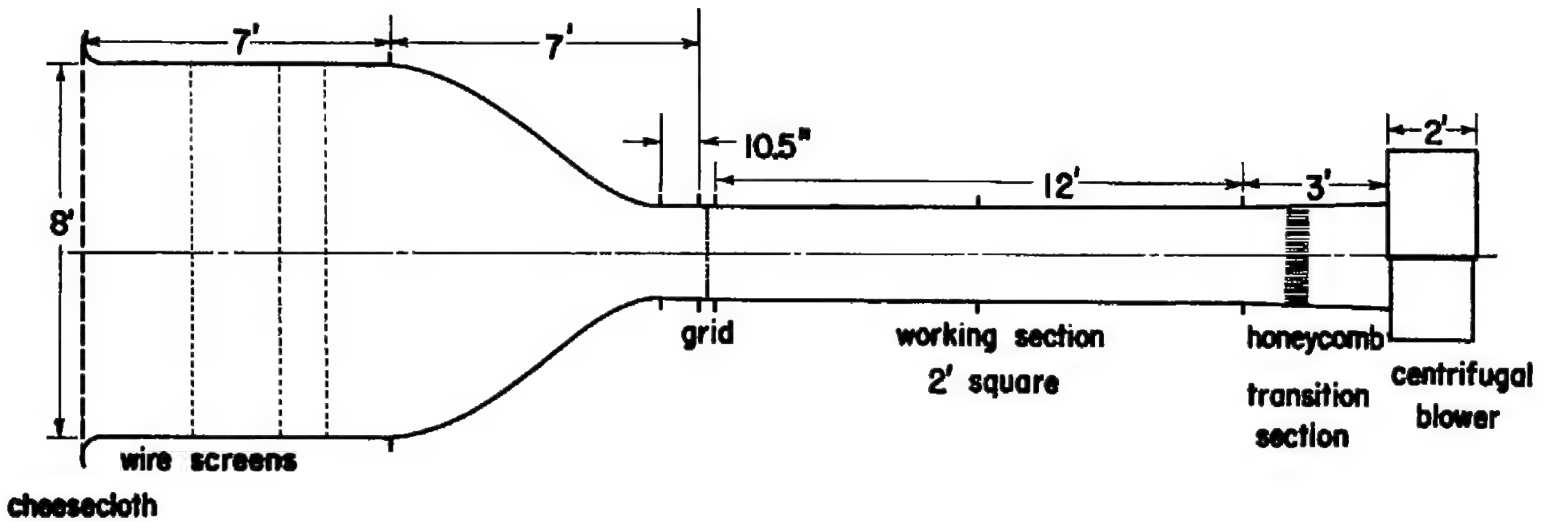

Figure 1.- Sketch of wind tunnel.

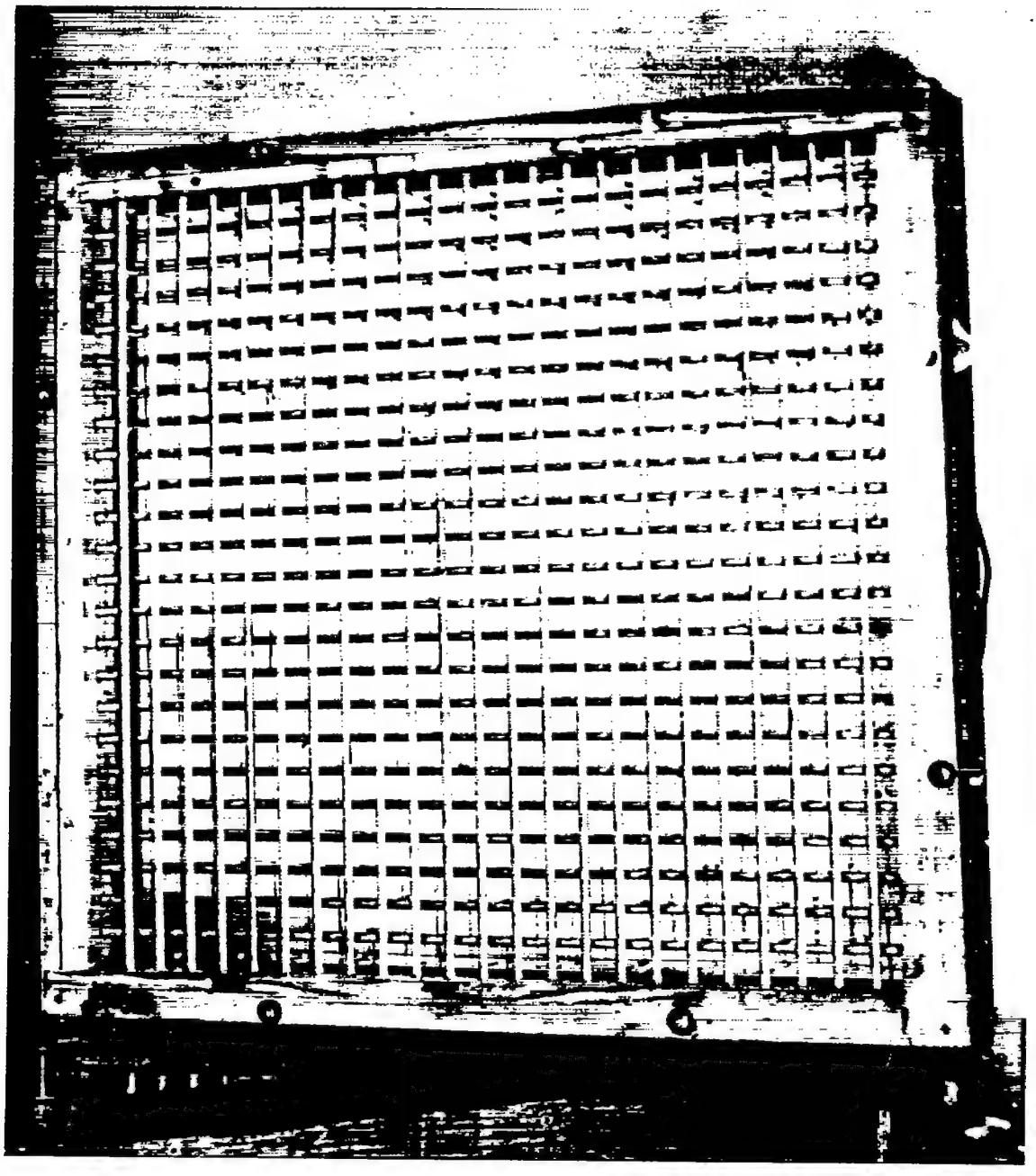

L-83689

Figure 2.- Hot grid photographed from downstream face. Parts of square heating mesh of double wires can be seen through wooden dowel grid.

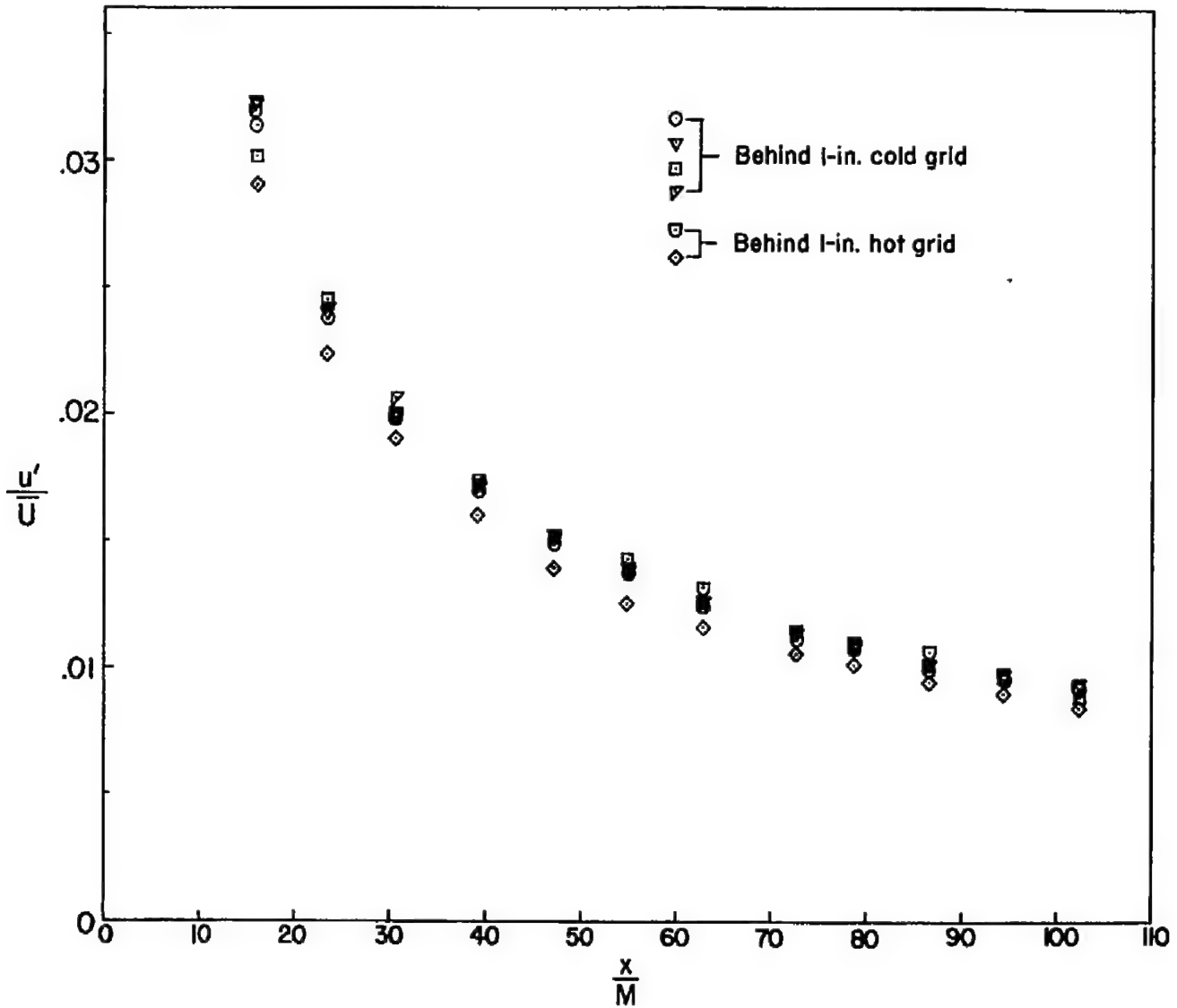

Figure 3.- Turbulence decay.

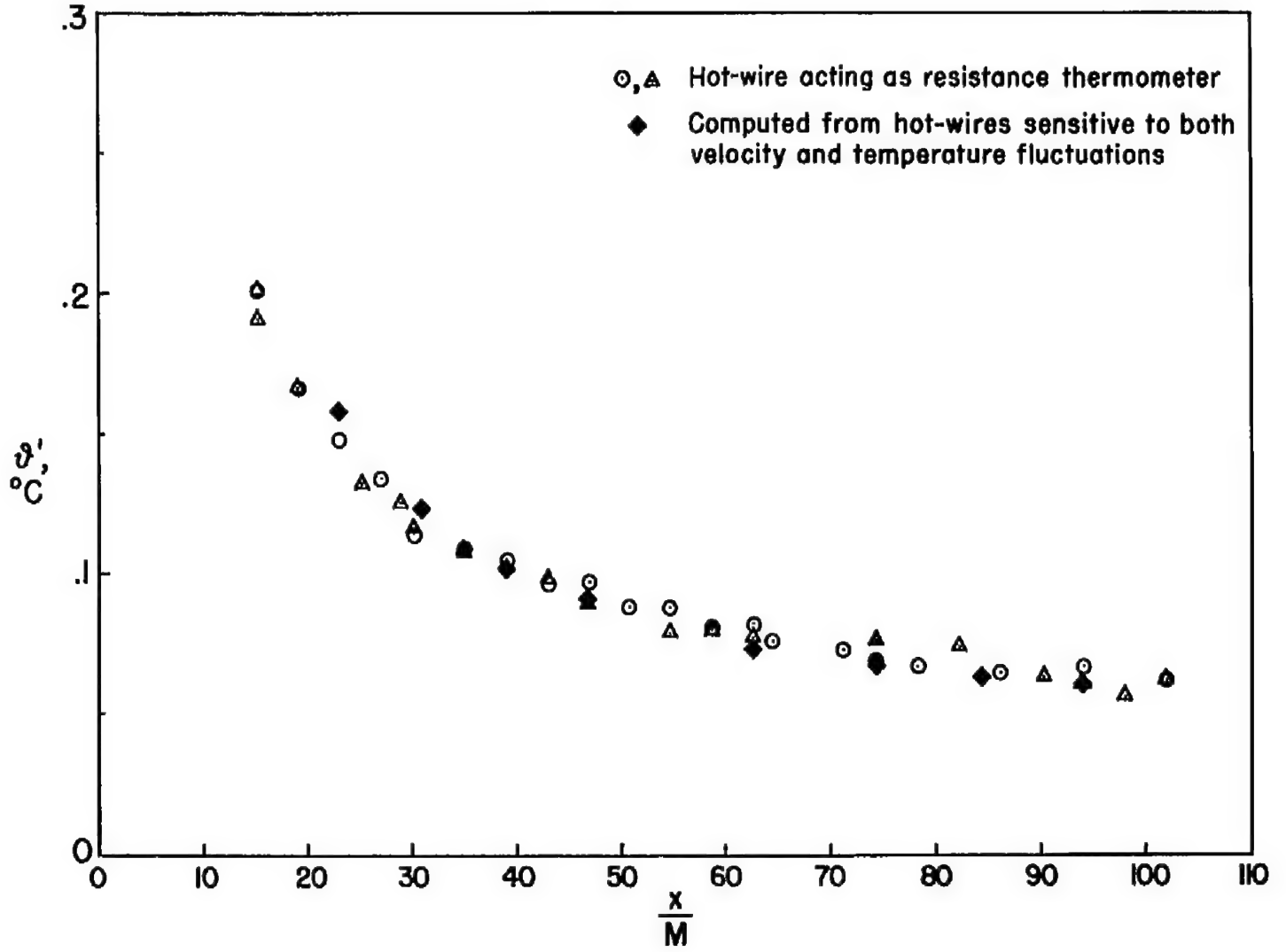

Figure 4.- Temperature fluctuation decay.

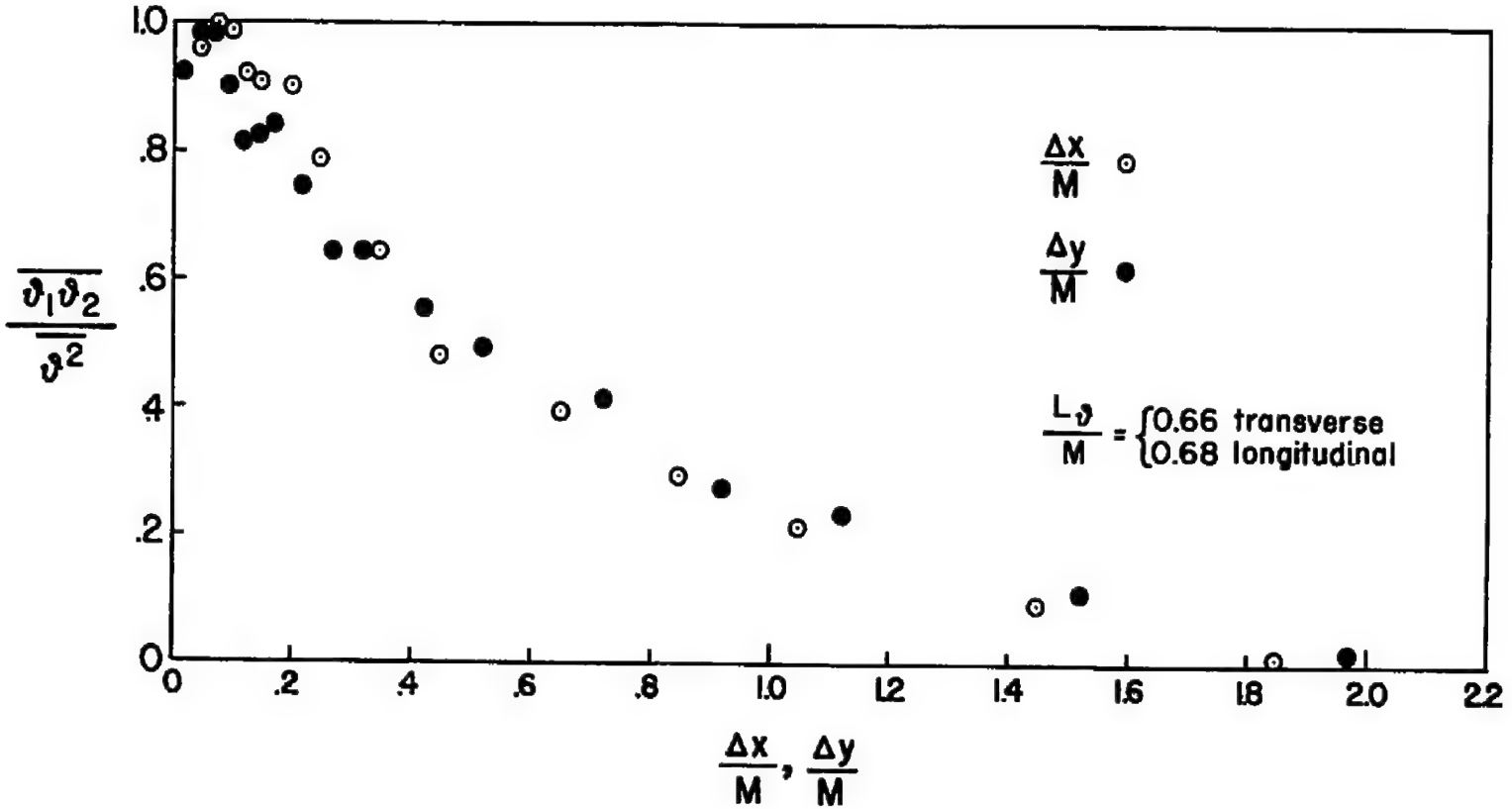

Figure 5.- Longitudinal and transversal temperature correlations.

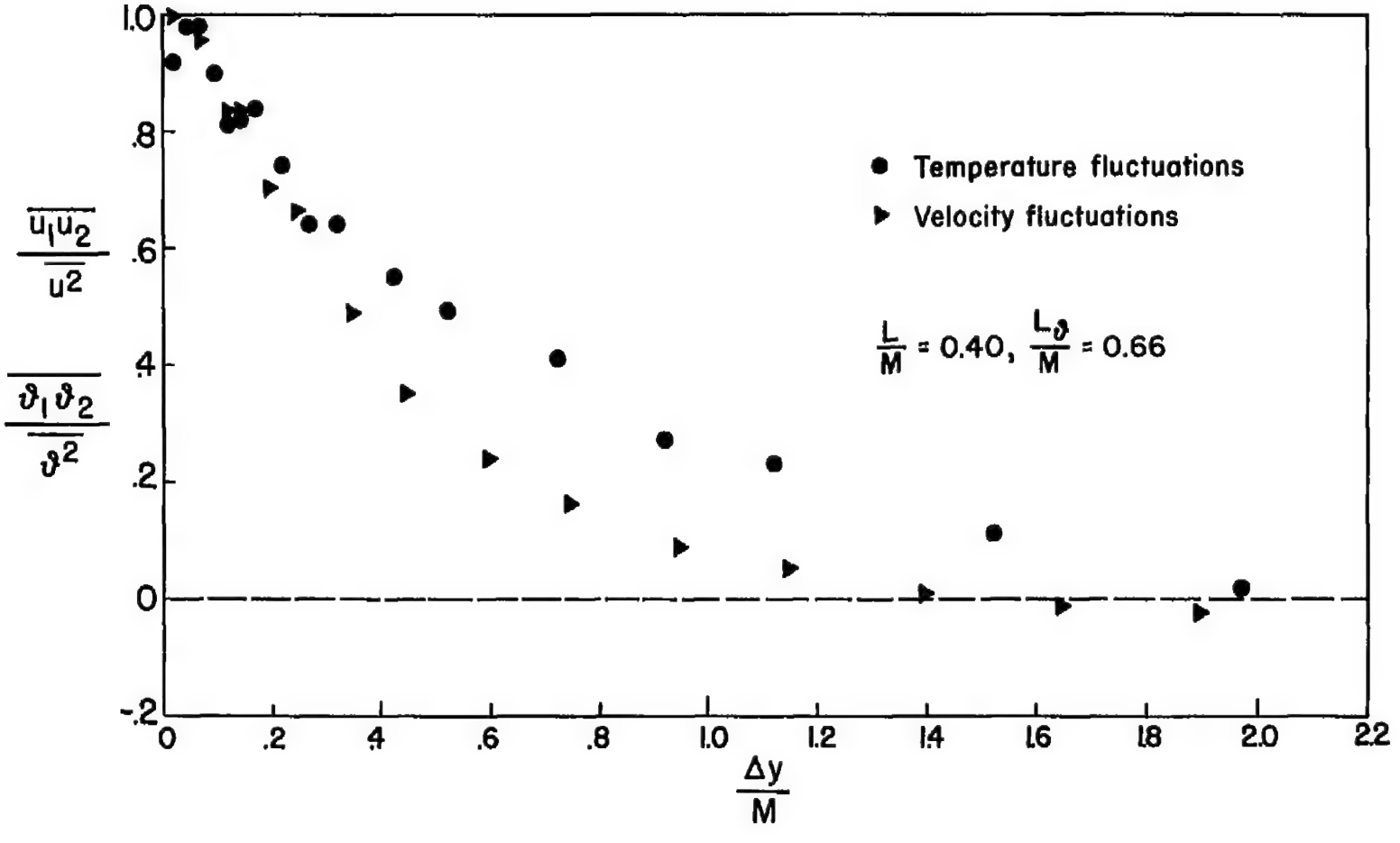

Figure 6.- Transversal velocity and temperature correlations.

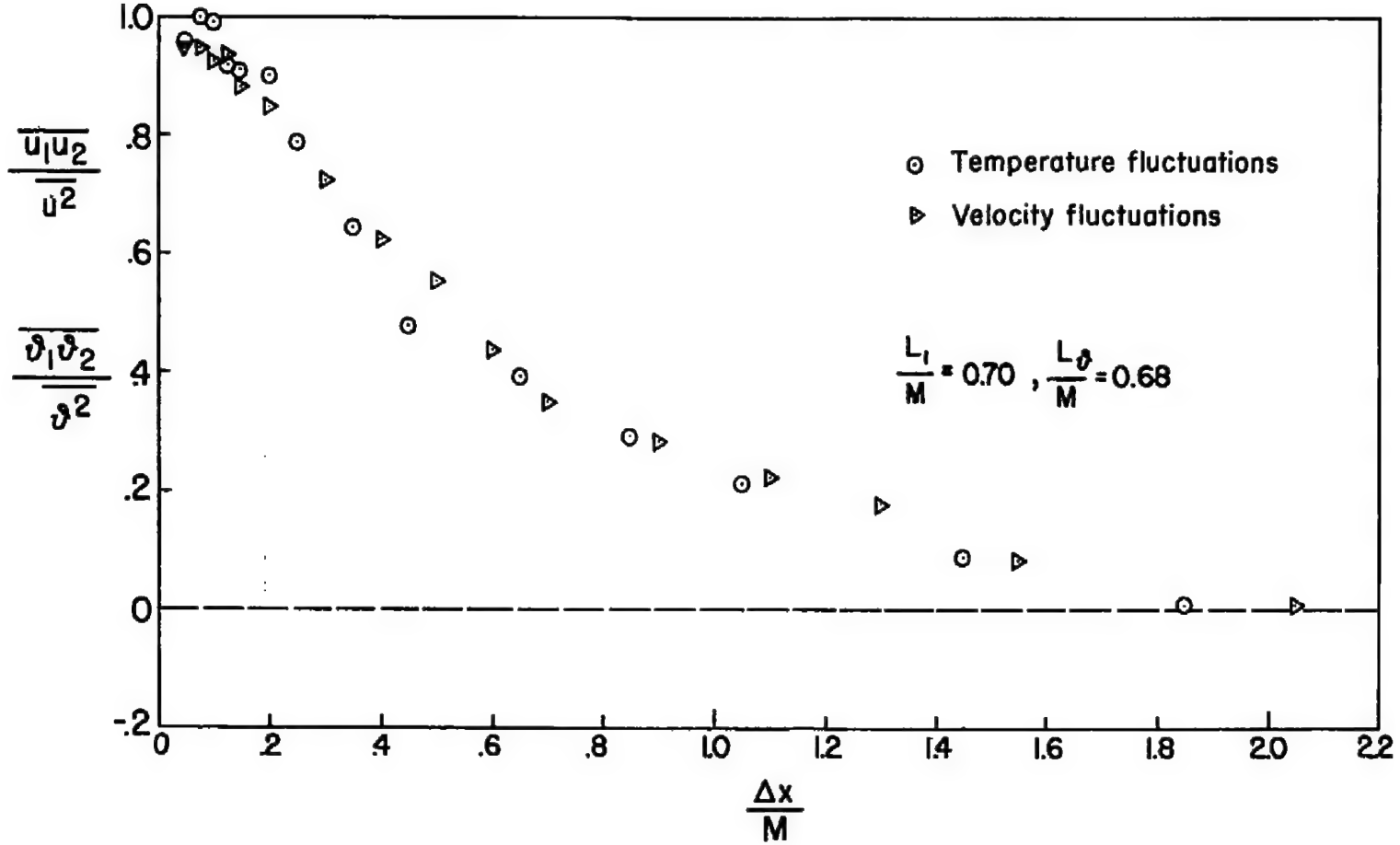

Figure 7.- Longitudinal velocity and temperature correlations.

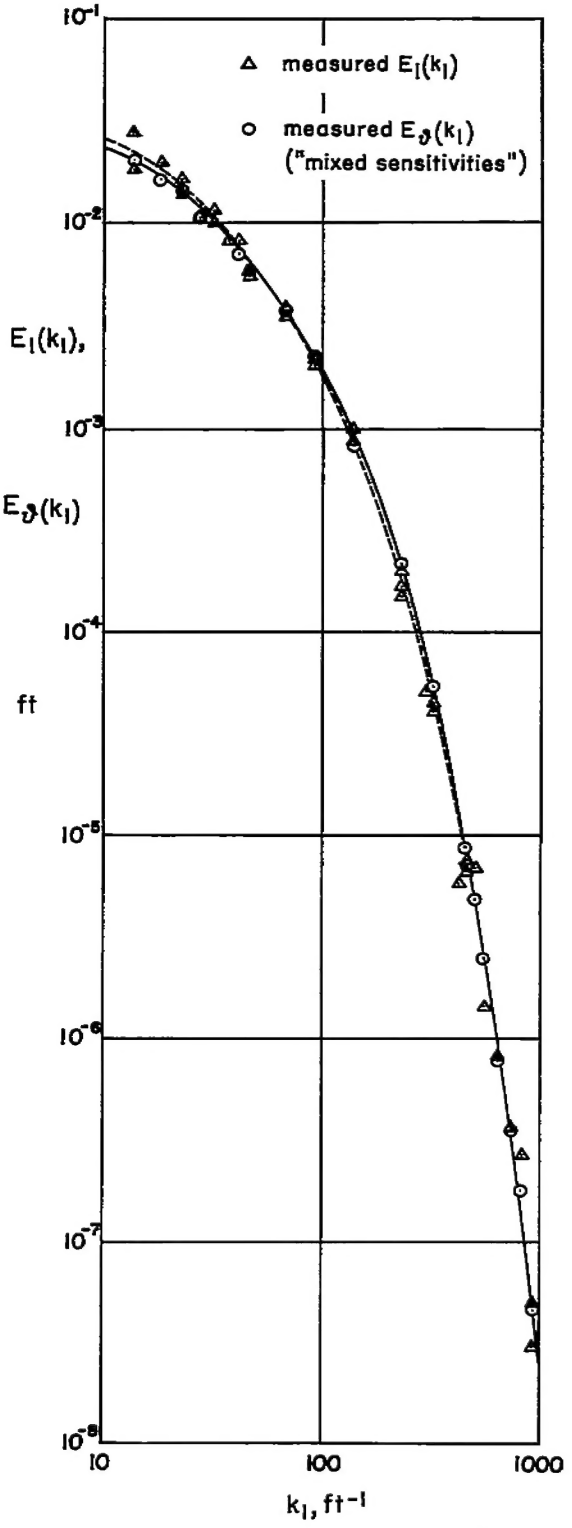

Figure 8.- u and ϑ spectra at x/M = 23.1.

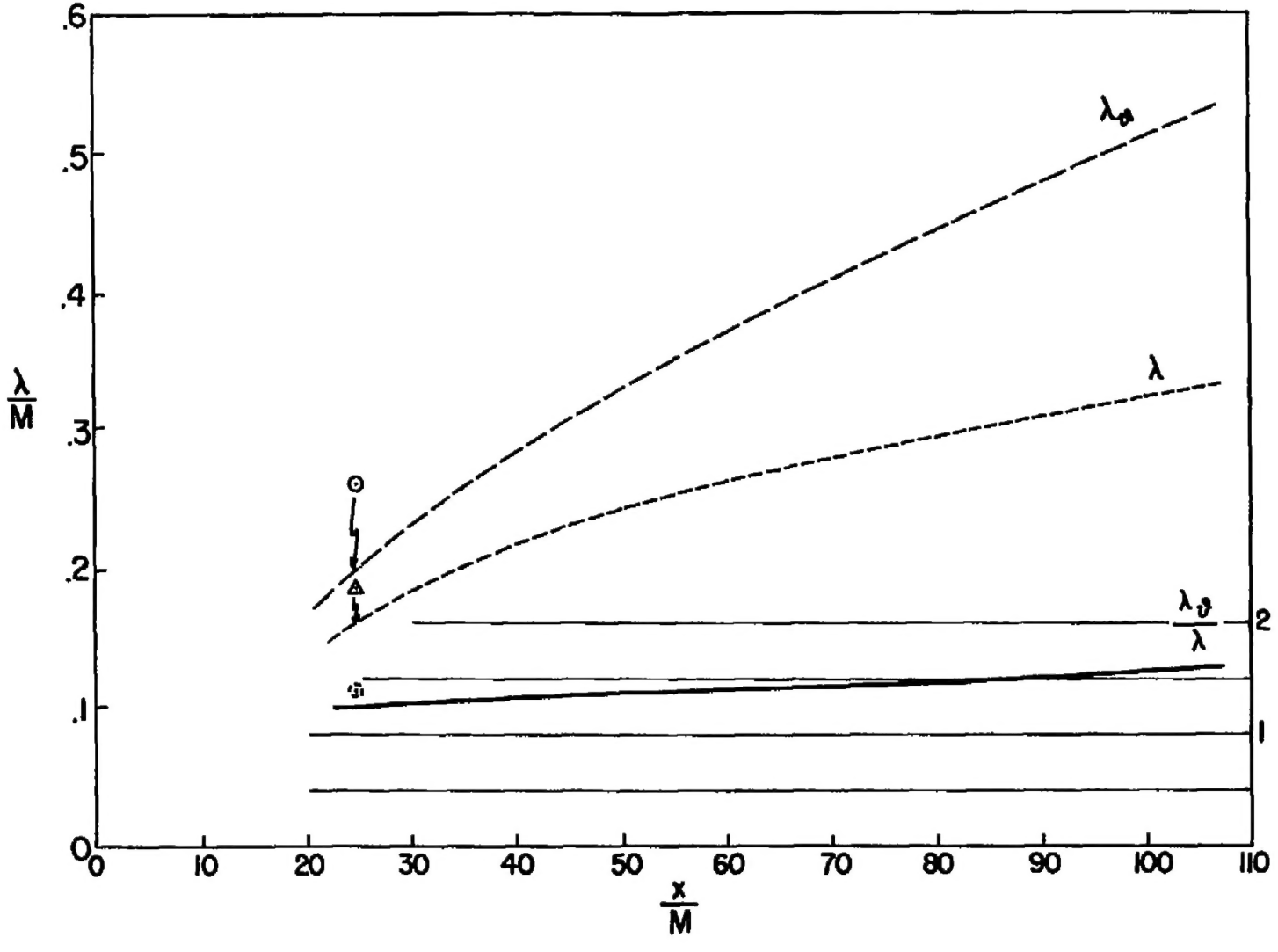

Figure 9.- λ's calculated from u' and ϑ' decay curves (points from measured spectra).

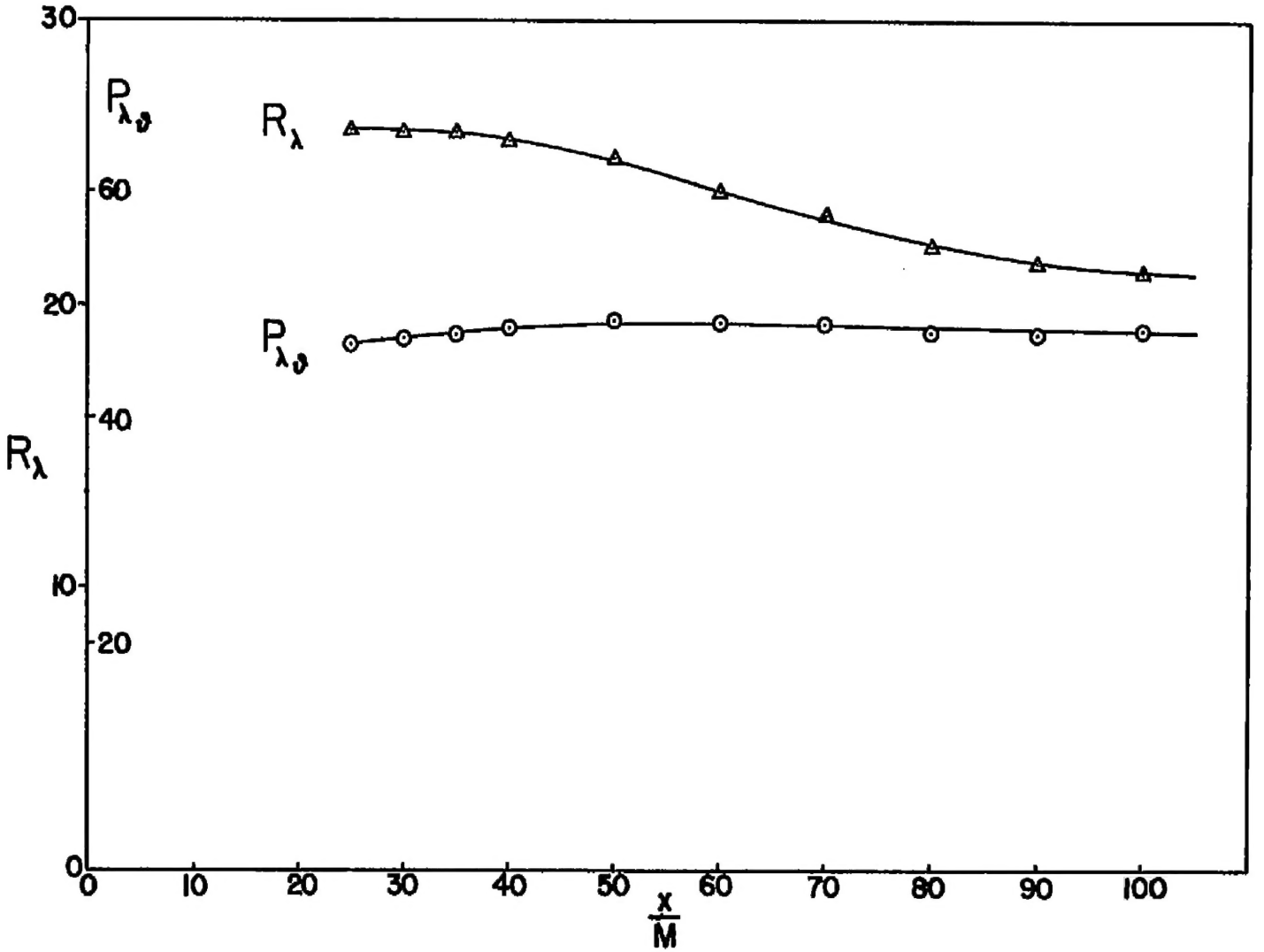

Figure 10.- Reynolds and Peclet numbers.

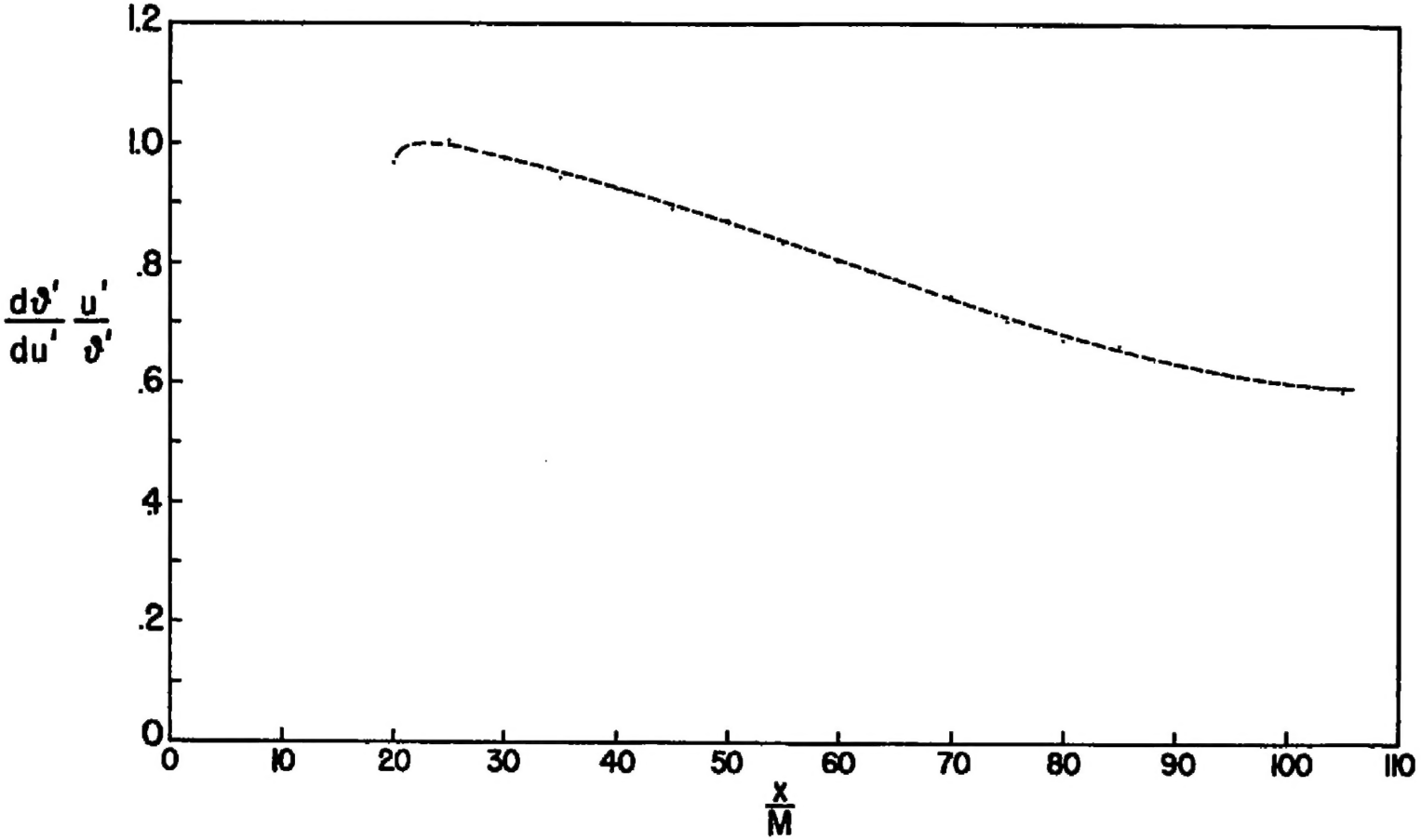

Figure 11.- Relative decay rates of u' and ϑ'.